ESMO GOOD SCIENCE BETTER MEDICINE BEST PRACTICE

ANNALS OF ONCOLOGY driving innovation in oncology

ORIGINAL ARTICLE

APOBEC mutagenesis, kataegis, chromothripsis in *EGFR*-mutant osimertinib-resistant lung adenocarcinomas

P. Selenica[1†], A. Marra[1†], N. J. Choudhury[2†], A. Gazzo[1], C. J. Falcon[3], J. Patel[1], X. Pei[1], Y. Zhu[1], C. K. Y. Ng[4], M. Curry[5], G. Heller[5], Y.-K. Zhang[6], M. F. Berger[1,7,8], M. Ladanyi[8], C. M. Rudin[2,9], S. Chandarlapaty[1,9], C. M. Lovly[6], J. S. Reis-Filho[1*‡] & H. A. Yu[2,9*‡]

[1]Memorial Sloan Kettering Cancer Center, New York City; [2]Department of Medicine, Thoracic Oncology Service, Memorial Sloan Kettering Cancer Center, New York City; [3]Druckenmiller Center for Cancer Research, Memorial Sloan Kettering Cancer Center, New York City, USA; [4]Department for BioMedical Research (DBMR), University of Bern, Bern, Switzerland; [5]Department of Epidemiology and Biostatistics, Memorial Sloan Kettering Cancer Center, New York City; [6]Department of Medicine, Division of Hematology and Oncology and Vanderbilt-Ingram Cancer Center, Vanderbilt University Medical Center, Nashville; [7]Marie-Josée and Henry R. Kravis Center for Molecular Oncology, Memorial Sloan Kettering Cancer Center, New York City; [8]Department of Pathology, Molecular Diagnostics Service, Memorial Sloan Kettering Cancer Center, New York City; [9]Department of Medicine, Weill Cornell Medical College, New York City, USA

Available online 9 September 2022

Background: Studies of targeted therapy resistance in lung cancer have primarily focused on single-gene alterations. Based on prior work implicating apolipoprotein b mRNA-editing enzyme, catalytic polypeptide-like (APOBEC) mutagenesis in histological transformation of epidermal growth factor receptor (*EGFR*)-mutant lung cancers, we hypothesized that mutational signature analysis may help elucidate acquired resistance to targeted therapies.

Patients and methods: APOBEC mutational signatures derived from an Food and Drug Administration-cleared multigene panel [Memorial Sloan Kettering Cancer Center Integrated Mutation Profiling of Actionable Cancer Targets (MSK-IMPACT)] using the Signature Multivariate Analysis (SigMA) algorithm were validated against the gold standard of mutational signatures derived from whole-exome sequencing. Mutational signatures were decomposed in 3276 unique lung adenocarcinomas (LUADs), including 93 paired osimertinib-naïve and -resistant *EGFR*-mutant tumors. Associations between APOBEC and mechanisms of resistance to osimertinib were investigated. Whole-genome sequencing was carried out on available *EGFR*-mutant lung cancer samples (10 paired, 17 unpaired) to investigate large-scale genomic alterations potentially contributing to osimertinib resistance.

Results: APOBEC mutational signatures were more frequent in receptor tyrosine kinase (RTK)-driven lung cancers (*EGFR, ALK, RET,* and *ROS1;* 25%) compared to LUADs at large (20%, $P < 0.001$); across all subtypes, APOBEC mutational signatures were enriched in subclonal mutations ($P < 0.001$). In *EGFR*-mutant lung cancers, osimertinib-resistant samples more frequently displayed an APOBEC-dominant mutational signature compared to osimertinib-naïve samples (28% versus 14%, $P = 0.03$). Specifically, mutations detected in osimertinib-resistant tumors but not in pre-treatment samples significantly more frequently displayed an APOBEC-dominant mutational signature (44% versus 23%, $P < 0.001$). *EGFR*-mutant samples with APOBEC-dominant signatures had enrichment of large-scale genomic rearrangements ($P = 0.01$) and kataegis ($P = 0.03$) in areas of APOBEC mutagenesis.

Conclusions: APOBEC mutational signatures are frequent in RTK-driven LUADs and increase under the selective pressure of osimertinib in *EGFR*-mutant lung cancer. APOBEC mutational signature enrichment in subclonal mutations, private mutations acquired after osimertinib treatment, and areas of large-scale genomic rearrangements highlights a potentially fundamental role for APOBEC mutagenesis in the development of resistance to targeted therapies, which may be potentially exploited to overcome such resistance.

Key words: EGFR, mutational signatures, APOBEC, osimertinib, acquired resistance

*Correspondence to: Dr Helena A. Yu, Department of Medicine, Thoracic Oncology Service, Memorial Sloan Kettering Cancer Center, 545 E 73rd St, New York, NY 10021, USA. Tel: +1-(646)-608-3912

E-mail: yuh@mskcc.org (H. A. Yu).

*Dr Jorge S. Reis-Filho, Department of Pathology, Memorial Sloan Kettering Cancer Center, 1275 York Avenue, New York, NY 10021, USA. Tel: +1-(212)-639-8054

E-mail: reisfilj@mskcc.org (J. S. Reis-Filho).

†These authors contributed equally.

‡Co-corresponding authors.

INTRODUCTION

Most studies of resistance to targeted therapies have primarily focused on single-gene mutations or copy number alterations (CNAs) identified by multigene panel sequencing. In oncogene-driven lung cancers, a single-gene alteration that mediates resistance is rarely identified,[1] and only a subset of alterations detected are therapeutically actionable, with benefit limited by intratumoral heterogeneity and the subclonal nature of many of these acquired mutations.[2] Spatial and temporal mapping of therapeutic resistance at individual tumor sites suggests that subclonal alterations may be driven by large-scale mutational processes occurring during tumor evolution.[3-5] The contribution of genome-wide mutational processes in mediating tumor evolution and therapeutic resistance under the selective pressure of targeted therapies is underexplored. These large-scale patterns of mutagenesis drive genomic diversity and provide a substrate for clonal selection.[4] Merging layers of genomic interrogation, from base pair substitutions to large-scale chromosomal rearrangements, provides an integrated assessment of the adaptive processes that propagate resistance to targeted therapies in oncogene-driven lung cancers. Furthermore, as microsatellite instability and homologous recombination deficiency confer sensitivity to immune checkpoint inhibitors[6,7] and poly (ADP-ribose) polymerase (PARP) inhibitors,[8-10] respectively, other mutational signatures may provide the basis for the development of new therapeutic strategies in drug-resistant tumors.

Such additional interrogation may be particularly germane to lung cancers driven by epidermal growth factor receptor (*EGFR*) alterations. Patients with *EGFR*-mutant lung cancer are effectively treated with EGFR tyrosine kinase inhibitors (TKIs),[11] yet long-term disease control remains elusive. Acquired single-gene mutations and CNAs have been identified in only ∼20% of first-line osimertinib-resistant cases.[1] Lineage plasticity[1] and acquired structural rearrangements such as kinase gene fusions[12] are observed in about 25% of osimertinib-resistant tumors; these events are rarely seen in other oncogene-driven lung cancers. The mechanistic basis of the enrichment for these events in post-therapy *EGFR*-mutant lung cancers has yet to be defined. Prior work elucidating mechanisms of acquired resistance has focused on single-gene alterations; Catalogue of Somatic Mutations in Cancer (COSMIC) mutational signatures define larger genome-wide trends that may contribute to a better understanding of tumor initiation and evolution. We and others identified enrichment of large-scale genomic alterations such as apolipoprotein b mRNA-editing enzyme, catalytic polypeptide-like (APOBEC) mutational signatures in *EGFR*-mutant lung cancers destined for small-cell histologic transformation.[13,14] APOBEC signatures are one of the most prevalent mutational signatures in human cancers, derive from the activity of APOBEC cytosine deaminases, and have been implicated in tumorigenesis and potentially in therapeutic resistance.[15,16] APOBEC mutational signatures are also the dominant mutational signatures in lung adenocarcinomas (LUADs) with late-evolving subclonal driver alterations.[17]

Given these data, we hypothesized that APOBEC may have a causative role in mediating mechanisms of acquired resistance such as structural rearrangements and lineage plasticity seen in *EGFR*-mutant lung cancer. Validation of such a role would provide rationale for assessing APOBEC enzymatic inhibition in *EGFR*-mutant lung cancers. In the current study, we utilized an algorithm benchmarked for mutational signature detection in multigene sequencing panels[18] to examine the progression of APOBEC mutational signature levels in LUADs derived from clinically obtained multigene panel sequencing and whole-genome sequencing (WGS) to survey tumor evolution under the selective pressure of treatment.

METHODS

Study cohort

We identified all patients with LUAD with targeted hybrid capture, next-generation tumor sequencing (NGS) carried out at the Memorial Sloan Kettering Cancer Center (MSK) from March 2014 to March 2021 using the Food and Drug Administration (FDA)-approved MSK Integrated Mutation Profiling of Actionable Cancer Targets (MSK-IMPACT) assay NGS platform.[19,20] Clinical data collection, including patient demographics and treatments, was approved by the MSK Institutional Review Board/Privacy Board, and all patients provided written consent. Tumor samples were de-identified for further analyses. Of all patients with LUAD sequenced by MSK-IMPACT, 93 patients with *EGFR*-mutant lung cancer treated with osimertinib had available paired pre- and post-treatment tumor samples. For this subgroup, we collected demographic information, clinical characteristics, and detailed treatment histories, including line of treatment, time to treatment discontinuation on osimertinib, and overall survival (OS) from time of MSK-IMPACT, with left truncation adjustment.

Multigene panel sequencing, whole-genome sequencing, and mutational signature analysis

Somatic alterations were detected as described previously[19,20] utilizing the FDA-cleared New York State Department of Health-approved MSK-IMPACT, with a median sequencing coverage depth of 675x (range, 60x-1284x). CNAs and estimated tumor purity were identified using FACETS.[21] The cancer cell fraction (CCF) of each mutation was inferred using ABSOLUTE (v1.0.6), with the ABSOLUTE solutions manually reviewed.[22] Mutations were classified as clonal if the probability of the mutation being clonal was >0.5 or if the lower confidence interval (CI) was >0.9 as calculated by ABSOLUTE. To validate findings on MSK-IMPACT and provide further information regarding large-scale genomic rearrangements, WGS was carried out on pre- and/or post-osimertinib and matched normal tissue samples for 27 patients by MSK's Integrated Genomics Operations using validated protocols,[23,24] with a median

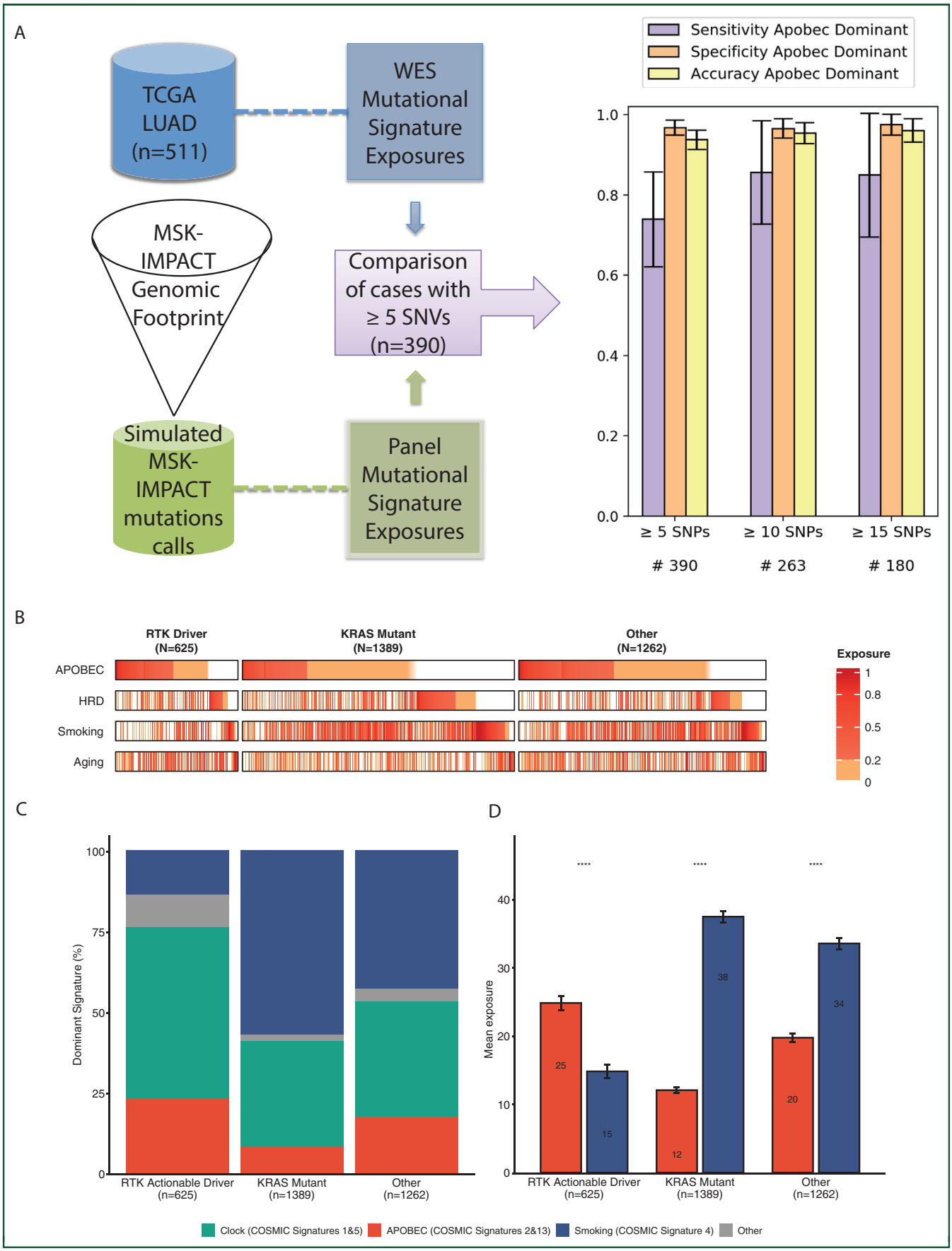

Figure 1. Mutational signatures derived from multigene panel sequencing. (A) Performance evaluation of SigMA comparing WES data from the TCGA LUAD cohort to that same data restricted to the MSK-IMPACT genomic footprint. Schematic demonstrating workflow for SigMA validation is shown on the left. Sensitivity, specificity, and accuracy are referred to the capacity of SigMA to detect APOBEC as the dominant mutational signature compared to the TCGA cohort. Performance is evaluated at cut-offs for samples with at least 5 SNVs, 10 SNVs, and 15 SNVs. (B) Mutational signature heatmap of lung adenocarcinomas ($n = 3276$) from the MSK-IMPACT

sequencing coverage depth of 57x (range, 48x-62x). WGS was completed on 6 pre-treatment, 11 post-treatment, and 10 paired samples derived from formalin-fixed, paraffin-embedded tissue samples or recaptured genomic DNA. Twenty of these patients also had either or both pre-/post-treatment samples analyzed by MSK-IMPACT. To evaluate the number and context type of somatic single-nucleotide variants (SNVs) acquired after osimertinib treatment between paired pre/post samples from the same patient, we calculated the fraction of substitutions that were private to the pre-osimertinib sample or private to the post-osimertinib sample. For each pair, all somatic SNVs that were detected in one sample were annotated to be either present (shared SNVs) or absent (private SNVs) in the other. To determine whether the potential contribution of artifacts stemmed from formalin fixation and paraffin embedding (i.e. primarily C>T SNVs), the frequency of SNV nucleotide changes was compared between pre- and post-treatment samples (Supplementary Table S1, available at https://doi.org/10.1016/j.annonc.2022.09.151), as well as across all mutations, mutations with <10% variant allele fraction, and mutations with <5% variant allele fraction (Supplementary Table S2, available at https://doi.org/10.1016/j.annonc.2022.09.151). Further description of methods is reported in the Supplementary methods, available at https://doi.org/10.1016/j.annonc.2022.09.151. In addition, given that recent studies have demonstrated that formalin fixation can leave predictable and identifiable mutational signatures across the genome (i.e. COSMIC SBS 30,[25]) we inspected the mutational profile of the formalin-fixed paraffin-embedded samples that were subjected to sequencing. No detectable levels of these specific signatures were identified (data not shown). Further description of methods is reported in the Supplementary methods, available at https://doi.org/10.1016/j.annonc.2022.09.151.

For MSK-IMPACT samples with at least five somatic SNVs, mutational signatures were computed using Signature Multivariate Analysis (SigMA),[18] a tool extensively benchmarked for the analysis of formalin-fixed paraffin-embedded samples subjected to multigene panel sequencing, as previously described.[26,27] A dominant signature for each sample was determined based on the proposed category assigned by SigMA, as previously reported.[18] The decomposed exposures (i.e. the fraction of mutations associated with a given mutational process) were converted into percentages to allow a meaningful comparison among samples with different numbers of mutations. Based on the decomposed exposure values, additional categories (i.e. APOBEC < or ≥20%) were computed and utilized in the downstream analyses carried out. The decision to adopt the cut-off of 20% was based on the lowest possible mutational signature exposure that can be detected with sufficient confidence in samples with ≥5 SNVs. In addition, SigMA was used to classify conventional codon-context mutation types for each variant. Classifications are based on the six substitution subtypes: C > A, C > G, C > T, T > A, T > C, and T > G, and the nucleotides immediately 5′ and 3′ to the mutation. Twelve APOBEC-context mutations were identified using the peaks present on the spectra of COSMIC Signature 2 and Signature 13 (4 and 8 codon-context mutations, respectively).

Evaluation of SigMA performance on MSK-IMPACT data

SigMA performance was evaluated using a simulation strategy to reproduce MSK-IMPACT samples from available whole-exome sequencing (WES) data from The Cancer Genome Atlas (TCGA; version mc3.v0.2.8) LUAD cohort. We considered the APOBEC exposures obtained from TCGA samples as ground truth. MSK-IMPACT sample simulation was carried out by filtering TCGA data for only those mutations occurring on regions covered by MSK-IMPACT. COSMIC mutational signatures were computed using SigMA and applying 'lung cancer' as reference tumor for both the simulated MSK-IMPACT samples and original TCGA WES samples. Performance was assessed using Pearson's coefficient, sensitivity, specificity, and accuracy. Cohen's kappa coefficient was used to assess the agreement between SigMA-proposed mutational signature categories, such as APOBEC <20% versus ≥20% and APOBEC dominant versus non-dominant.

Statistical analysis

Statistical analyses were conducted using R (version 3.1.2). Comparisons of categorical and continuous variables were carried out by Fisher's exact and Mann—Whitney *U* tests, respectively. Differences in mutational signature exposures across multiple groups were analyzed using the Mann—Whitney *U* test. Pearson's correlation was used to compare mutational signature exposures. Oncoplots for mutational landscape visualization and heatmaps were created using the R packages maftools[28] and ComplexHeatmap,[29] respectively. Comparisons of frequencies of genes altered by somatic genetic alterations (including non-synonymous mutations, gene amplifications, and/or homozygous deletions) between either pre- and post-osimertinib samples or different APOBEC exposure cut-offs (<20% versus ≥20%) were carried out using Fisher's exact test. Comparative analysis in paired samples was carried out by the Wilcoxon signed rank test. Mutation

cohort. Exposure of mutational signatures for each sample according to the group [RTK driver ($n = 625$), *KRAS* mutant ($n = 1389$), Other ($n = 1262$)]. Exposures are reported as continuous variables and colored according to the legend (0 = white; 0.01-0.19 = orange shades; 0.2-1.0 = red shades). (C) Stacked bar plots of dominant signatures across RTK driver, *KRAS* mutant, and Other groups. Dominant signature was selected according to the category assigned by SigMA. (D) Comparison of APOBEC and smoking-related mutational signature exposures between RTK driver, *KRAS* mutant, and Other groups. The mean exposures attributed to smoking and APOBEC processes are plotted with error bars indicating standard deviations. Mutational signatures are color coded according to the legend. Statistical comparisons were carried out using two-sided Wilcoxon-Mann—Whitney test. RTK driver was considered as the reference group. **** = $P < 0.001$.

APOBEC, apolipoprotein b mRNA-editing enzyme, catalytic polypeptide-like; LUAD, lung adenocarcinoma; MSK-IMPACT, Memorial Sloan Kettering Cancer Center Integrated Mutation Profiling of Actionable Cancer Targets; RTK, receptor tyrosine kinase; SNV, single-nucleotide variants; TCGA, The Cancer Genome Atlas; WES, whole-exome sequencing.

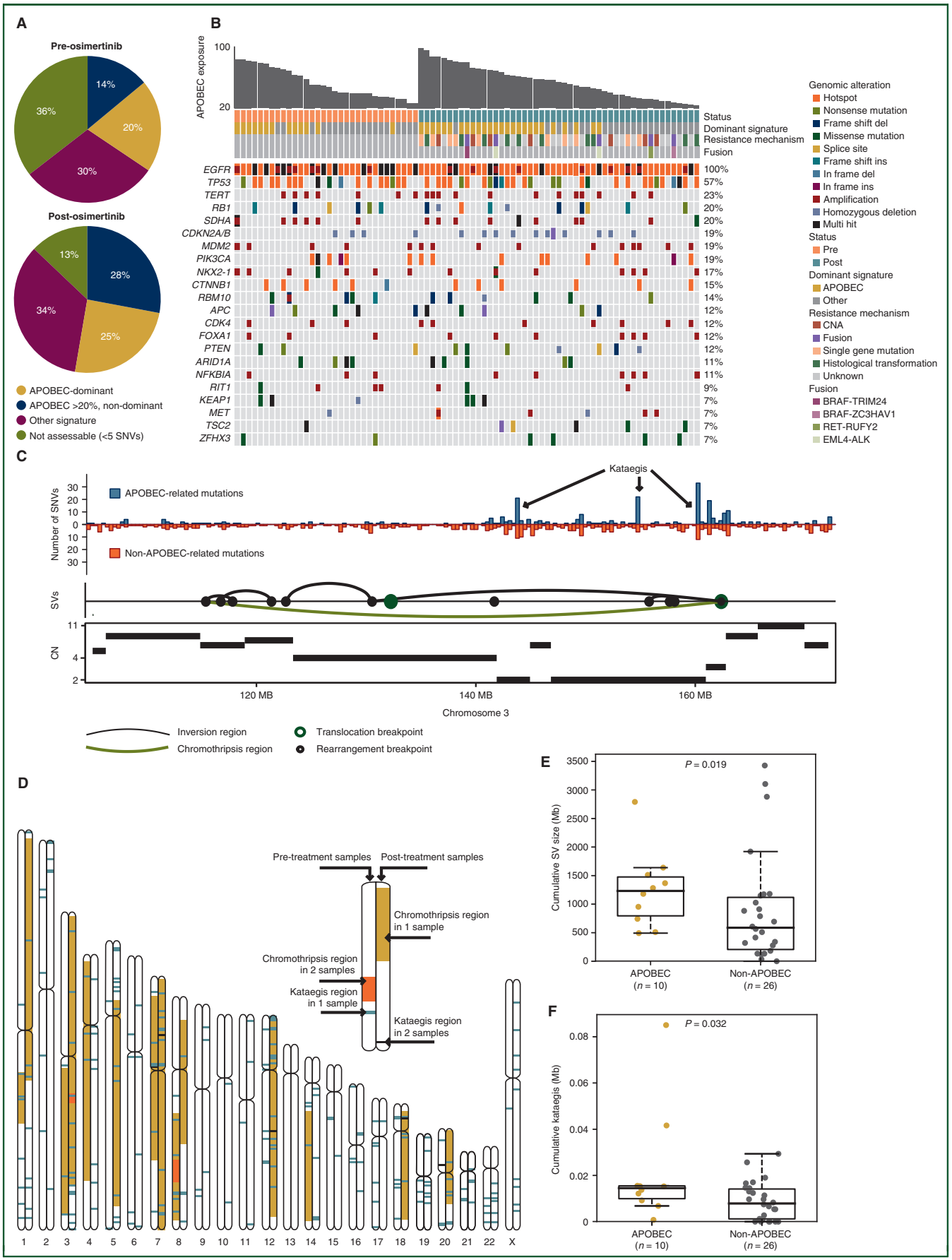

Figure 2. APOBEC mutagenesis in *EGFR*-mutant lung adenocarcinomas treated with osimertinib. (A) Pie charts showing the proportions of cases with APOBEC dominant, APOBEC mutational signature exposure > 20% but non-dominant, Other, and not assessable (<5 SNVs) signatures between pre- (n = 93) and

frequencies related to APOBEC mutagenesis in the kataegis and non-kataegis areas were compared using Fisher's exact test. Multiple testing correction using the Benjamini–Hochberg method was applied to control for the false discovery rate whenever appropriate. $P < 0.05$ was considered statistically significant. All tests were two-tailed.

RESULTS

Mutational signatures can be accurately derived from targeted sequencing data

Since only a small fraction of patient samples undergo WES or WGS, we first sought to validate the performance of the SigMA algorithm in calling APOBEC mutational exposures from the MSK-IMPACT-targeted gene panel, which is ordered routinely for clinical purposes as an integral element of patient care at MSKCC. WES data from the TCGA LUAD cohort ($n = 511$) served as a benchmark. MSK-IMPACT simulation was carried out by the inclusion of SNVs encompassed by the genomic footprint of MSK-IMPACT; only samples with $\geq$5 SNVs were included, as required by the SigMA algorithm ($n = 390$) (Figure 1A). We evaluated two methods for identifying APOBEC-enriched samples in the MSK-simulated cohort: those with POBEC identified as dominant mutational signature by SigMA mutational analysis (i.e. the mutational process with the highest level of exposure) and those with high levels of APOBEC exposure, arbitrarily defined as $\geq$20% exposure. The concordance between each of these designations was tested by signature analysis of the TCGA WES cohort (ground truth). SigMA detected APOBEC as dominant signature in MSK-IMPACT-simulated samples with 74% sensitivity and 97% specificity (Figure 1A). Sensitivity increased to 86% and 85%, respectively, when $\geq$10 and $\geq$15 mutations were included with 97% specificity in both groups. Using Cohen's kappa correlation test, we observed a substantial agreement (K scores 0.72-0.81) in detecting APOBEC as dominant mutational signature between WES and MSK-IMPACT-simulated panel (Supplementary Table S3, available at https://doi.org/10.1016/j.annonc.2022.09.151). Detection of APOBEC exposure $\geq$ 20% yielded comparable metrics (Supplementary Figure S1A, available at https://doi.org/10.1016/j.annonc.2022.09.151). When considered as a continuous variable, APOBEC exposure was highly correlated between TCGA WES and MSK-IMPACT-simulated samples (Pearson's $r = 0.77$, $P < 0.0001$; Supplementary Figure S1B, available at https://doi.org/10.1016/j.annonc.2022.09.151). As additional validation, mutational signatures were computed by SigMA in 18 samples for which both WGS and MSK-IMPACT data were available. A significant positive correlation between APOBEC mutational signature exposures detected by MSK-IMPACT and WGS was observed (Pearson's $r = 0.91$, $P < 0.0001$; Supplementary Figure S1C, available at https://doi.org/10.1016/j.annonc.2022.09.151). These results show the consistency and reliability of SigMA in detecting APOBEC mutational signatures in LUAD samples sequenced by the MSK-IMPACT gene panel. Given the higher concordance observed between APOBEC-dominant signature calling between TCGA WES and MSK-IMPACT-simulated cohort ($K = 0.72$), this designation was selected for subsequent analysis.

APOBEC mutational signature is enriched in RTK-driven LUADs

We next sought to analyze the frequency of APOBEC mutational signatures in a large cohort of LUADs. We identified 6034 LUAD samples which had undergone targeted gene sequencing with MSK-IMPACT; 3276 samples contained the requisite of $\geq$5 SNVs required for SigMA signature analysis. Tumors were first sorted according to known oncogenic drivers. We created an RTK driver subgroup encompassing four well-characterized receptor tyrosine kinase (RTK) driver alterations in *EGFR*, *ALK*, *RET*, and *ROS1*, all of which have approved targeted therapies and are enriched in patients with little or no smoking history (Figure 1B). *KRAS*-mutant lung cancers were selected as a molecularly defined comparator that occur more commonly in patients with smoking histories. The remaining LUADs were classified into the 'Other' category.

Mutational signature analysis revealed that APOBEC mutational signatures were more frequently identified as the dominant signature in the RTK driver group (23%) compared to both the *KRAS* (8%, $P < 0.001$) and Other subgroups (17%, $P < 0.001$) (Figure 1C). Conversely, smoking signature was more frequently the dominant signature in the *KRAS* subgroup (57%) compared to both the RTK driver (14%, $P < 0.001$) and Other (43%, $P < 0.001$) subgroups. The RTK driver subgroup also displayed the highest mean APOBEC mutational signature exposure (25% versus 20% in Other, $P < 0.001$, and 12% in *KRAS*, $P < 0.001$, Figure 1D). To take into account potential biases related to the threshold of $\geq$5 SNVs for SigMA signature analysis, a sensitivity analysis using higher cut-offs was carried out. A numeric increment in the proportion of cases with APOBEC as dominant mutational signature was found in the RTK driver group when the $\geq$10 and $\geq$15 SNVs thresholds were adopted (43% and 54%, respectively; Supplementary Figure S2A-C, available at https://doi.org/10.1016/j.annonc.2022.09.151). This trend,

post-osimertinib ($n = 93$) samples. (B) Repertoire of somatic genetic alterations of lung adenocarcinomas treated with osimertinib harboring APOBEC mutational signature $\geq$ 20% (pre = 32; post = 49). APOBEC mutational signature exposure, treatment status (pre- versus post-osimertinib), dominant mutational signature (APOBEC versus Other), and acquired resistance mechanism for each sample are represented and color coded according to the legend. (C) Region of overlap of chromothripsis and kataegis on chromosome 3 for a single sample with osimertinib resistance (WGS-Post01). APOBEC and non-APOBEC SNVs (top) are shown along with regions of kataegis, SVs (upper-middle) with inversions as black dots connected by curved lines, and translocations as green dots. A green curved line encompasses the segment of the chromosome that has undergone chromothripsis (middle). Integer CN of segments of chromosome 3 are shown in the bottom graph. (D) Genomic footprint of kataegis and chromothripsis across pre- and post-treatment whole-genome sequenced samples ($n = 36$). (E) Quantification of SVs and (F) kataegis across the genome in APOBEC dominant whole-genome sequenced samples as compared to APOBEC non-dominant. Statistical comparisons were carried out using two-sided Wilcoxon-Mann–Whitney test.

APOBEC, apolipoprotein b mRNA-editing enzyme, catalytic polypeptide-like; CN, copy number; EGFR, epidermal growth factor receptor; SNVs, single-nucleotide variants; SVs, structural variants.

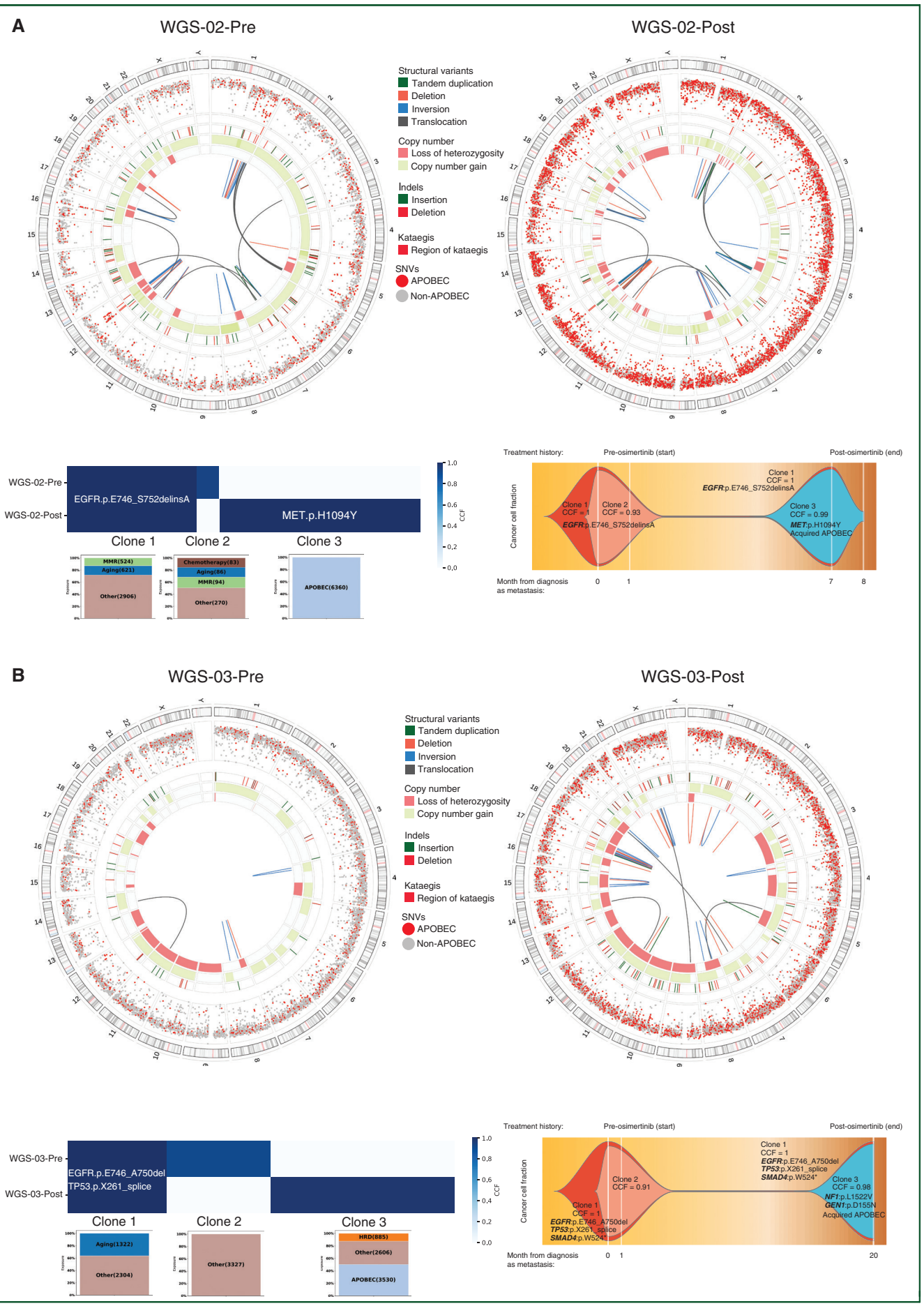
A
WGS-02-Pre
WGS-02-Post
Structural variants
Tandem duplication
Deletion
Inversion
Translocation
Copy number
Loss of heterozygosity
Copy number gain
Indels
Insertion
Deletion
Kataegis
Region of kataegis
SNVs
APOBEC
Non-APOBEC
WGS-02-Pre
WGS-02-Post
EGFR.p.E746_S752delinsA
MET.p.H1094Y
CCF
Clone 1
Clone 2
Clone 3
MMR(524)
Aging(621)
Other(2906)
Chemotherapy(83)
Aging(86)
MMR(94)
Other(270)
APOBEC(6360)
Treatment history:
Pre-osimertinib (start)
Post-osimertinib (end)
Cancer cell fraction
Clone 1
CCF = 1
EGFR:p.E746_S752delinsA
Clone 2
CCF = 0.93
EGFR:p.E746_S752delinsA
Clone 1
CCF = 1
EGFR:p.E746_S752delinsA
Clone 3
CCF = 0.99
MET:p.H1094Y
Acquired APOBEC
Month from diagnosis as metastasis:
0
1
7
8
B
WGS-03-Pre
WGS-03-Post
Structural variants
Tandem duplication
Deletion
Inversion
Translocation
Copy number
Loss of heterozygosity
Copy number gain
Indels
Insertion
Deletion
Kataegis
Region of kataegis
SNVs
APOBEC
Non-APOBEC
WGS-03-Pre
WGS-03-Post
EGFR.p.E746_A750del
TP53.p.X261_splice
CCF
Clone 1
Clone 2
Clone 3
Aging(1322)
Other(2304)
Other(3327)
HRD(885)
Other(2606)
APOBEC(3530)
Treatment history:
Pre-osimertinib (start)
Post-osimertinib (end)
Cancer cell fraction
Clone 1
CCF = 1
EGFR:p.E746_A750del
TP53:p.X261_splice
SMAD4:p.W524*
Clone 2
CCF = 0.91
Clone 1
CCF = 1
EGFR:p.E746_A750del
TP53:p.X261_splice
SMAD4:p.W524*
Clone 3
CCF = 0.98
NF1:p.L1522V
GEN1:p.D155N
Acquired APOBEC
Month from diagnosis as metastasis:
0
1
20

however, was not observed in the KRAS (11% and 15% using $\geq$10 and $\geq$15 SNVs, respectively) and Other (20% and 20% using $\geq$10 and $\geq$15 SNVs, respectively) groups where the proportions of APOBEC-dominant cases remained constant even if different SNV cut-offs were applied. Conversely, we observed an increment in the proportion of smoking signature in the KRAS (57%, 71%, and 75% using $\geq$5, $\geq$10, and $\geq$15 SNVs, respectively) and Other (43%, 57%, and 64% using $\geq$5, $\geq$10, and $\geq$15 SNVs, respectively) groups when higher SNV thresholds were applied (Supplementary Figure S2A-C, available at https://doi.org/10.1016/j.annonc.2022.09.151). These findings remained consistent when the proportions of the mutational exposures were tested rather than dominant signatures (Supplementary Figure S2D-F, available at https://doi.org/10.1016/j.annonc.2022.09.151). The smoking signature was inversely correlated with APOBEC signature (Pearson's r = −0.36, $P < 0.001$; Supplementary Figure S3A, available at https://doi.org/10.1016/j.annonc.2022.09.151), which was observed consistently across all subgroups. In a univariable model, RTK driver tumors were significantly more likely to have APOBEC as a dominant signature compared to *KRAS*-mutant tumors [odds ratio (OR) 0.30 for *KRAS* compared to RTK, 95% CI 0.23-0.39, $P < 0.001$] and Other (OR 0.72 for Other compared to RTK, 95% CI 0.57-0.91, $P < 0.001$, Supplementary Table S4, available at https://doi.org/10.1016/j.annonc.2022.09.151), although results in a multivariate analysis accounting for age, sex, smoking status, and sample type (primary versus metastatic) did not reach statistical significance (Supplementary Table S5, available at https://doi.org/10.1016/j.annonc.2022.09.151). These findings support the notion that APOBEC mutational signatures are significantly enriched in RTK-driven LUADs.

We further evaluated the proportion of APOBEC-site mutations by clonal status in cases with APOBEC as the dominant mutational signature compared to non-dominant. APOBEC-site mutations were detected more frequently at the subclonal rather than the clonal level in LUADs displaying dominant APOBEC signature in all considered subgroups ($P < 0.001$; Supplementary Figure S3B, available at https://doi.org/10.1016/j.annonc.2022.09.151), consistent with previous findings that have associated APOBEC mutagenesis with the acquisition of subclonal mutations.[3,30]

We also assessed spatial and temporal evolution of mutational signatures in LUAD samples from primary (from lung tissue) or metastatic (from tissue other than lung) sites; site of tumor was available for 3248/3276 samples (Supplementary Figure S3C, available at https://doi.org/10.1016/j.annonc.2022.09.151). Metastatic tumors ($n = 1364$) exhibited a significantly higher mean APOBEC exposure compared to lung primaries ($n = 1884$, 21% versus 15%, $P < 0.001$, Supplementary Figure S3D, available at https://doi.org/10.1016/j.annonc.2022.09.151), a pattern conserved across all three molecular subgroups (Supplementary Figure S3E, available at https://doi.org/10.1016/j.annonc.2022.09.151). These data support a modest yet statistically significant enrichment in APOBEC signatures in metastatic tumors, suggesting that APOBEC may constitute a relatively late event in the development and progression of LUADs.[31]

Evolution of mutational signatures with osimertinib treatment in EGFR-mutant lung cancers

To evaluate the evolution of APOBEC mutational signature with the selective pressure of targeted therapy, we identified 93 patients with paired osimertinib-naïve and osimertinib-resistant tumor samples that underwent MSK-IMPACT sequencing. Fifty-two received osimertinib as first-line treatment and 41 as later-line treatment. Sixty osimertinib-naïve and 81 osimertinib-resistant tumors had the requisite $\geq$5 SNVs; 54 patients had both samples meet this criterion. APOBEC was the dominant signature in twice as many osimertinib-resistant samples compared with osimertinib-naïve samples (28% versus 14%, $P = 0.03$, Figure 2A, Supplementary Figure S4A, available at https://doi.org/10.1016/j.annonc.2022.09.151). Numerically higher APOBEC exposure was also detected in osimertinib-resistant tumors compared to matched osimertinib-naïve samples (Wilcoxon signed rank test, $P = 0.33$, Supplementary Figure S4B, available at https://doi.org/10.1016/j.annonc.2022.09.151). Somatic tumor mutational burden (TMB) was also higher in post-osimertinib compared to pre-osimertinib samples, suggesting a possible correlation between APOBEC mutagenesis and TMB ($P < 0.001$, Supplementary Figure S4C, available at https://doi.org/10.1016/j.annonc.2022.09.151).

To ascertain the contribution of APOBEC mutagenesis to the mutations acquired after treatment with osimertinib, we analyzed 10 cases with paired osimertinib-naïve and -resistant samples that underwent WGS. Interestingly, we found that the proportion of APOBEC-site mutations private to post-treatment samples was significantly higher than those shared with pre-treatment samples (44% versus 23%, $P < 0.001$, Supplementary Figure S4D, available at https://doi.org/10.1016/j.annonc.2022.09.151). These data suggest that a high proportion of *EGFR*-mutant lung tumors have evidence of *de novo* APOBEC activity before treatment, with further enrichment in APOBEC-driven mutagenesis and acquired APOBEC-context mutations following osimertinib.

Concurrent alterations on MSK-IMPACT and mutational signatures

To evaluate whether recurrent mutations in common somatic hotspots might be associated with APOBEC mutagenesis, we focused on cases with both dominant APOBEC

Figure 3. Large-scale molecular patterns detected by WGS in *EGFR*-mutant lung adenocarcinomas. (A) Circos plot of pre-treatment (top left) and post-treatment (top right) displaying (from inside to outside) inter-variant distance and APOBEC classification of SNVs, regions of kataegis, indels, copy number, and structural variants of WGS-02-Pre/Post osimertinib and (B) WGS-03-Pre/Post. Clonality heatmap (bottom left) and fishtail plot (bottom right) showing CCFs, mutations of interest, and mutational signatures in bioinformatically inferred clones.

APOBEC, apolipoprotein b mRNA-editing enzyme, catalytic polypeptide-like; CCFs, cancer cell fractions; EGFR, epidermal growth factor receptor; SNVs, single-nucleotide variants.

mutational signature as well as high exposure. There was no specific pattern of concurrent alterations identified in osimertinib-resistant samples in tumors with APOBEC as the dominant signature (Figure 2B). Similarly, no statistically significant enrichment in gene alterations was found when considering tumors with high APOBEC exposure ($\geq$20%) as compared to no exposure. No significant changes in CNAs were found between osimertinib-naïve and -resistant samples when stratifying by APOBEC mutational signature $<$20% versus $\geq$20% (Supplementary Figure S4E and F, available at https://doi.org/10.1016/j.annonc.2022.09.151). These findings indicate that APOBEC mutagenesis is unlikely to be involved in the development of canonical resistance SNVs or CNAs, such as EGFR C797S or *MET* amplification.

APOBEC and its relationship with large-scale chromosomal changes

Previous reports demonstrate that APOBEC-dependent kataegis and chromothripsis[32] provide a potential etiology for large-scale chromosomal rearrangements in the setting of APOBEC mutagenesis, prompting an interest in investigating the potential relationship between structural rearrangements and APOBEC mutagenesis. Kataegis describes a pattern of localized hypermutation within a cancer genome, while chromothripsis is a mutational process where thousands of chromosomal rearrangements occur in a single event clustered in a confined genomic region.[33] A subset of patients had sufficient tissue to perform WGS (10 paired pre/post samples, 6 pre only, 11 post only). In specific cases, kataegis and chromothripsis coincided with areas of the genome enriched with APOBEC mutations, as shown with case WGS-01 (Figure 2C). Collectively, when assessing all WGS samples, large-scale genomic rearrangements including kataegis and chromothripsis were dispersed uniformly across the genome (Figure 2D). Interestingly, tumors displaying dominant APOBEC signature had a statistically significant enrichment of the genome covered by structural variants ($P < 0.01$; Figure 2E) and kataegis ($P < 0.03$; Figure 2F).

We analyzed matched samples before and after osimertinib treatment to characterize the tumor evolution under therapeutic selection. Case WGS-02 (Figure 3A) was derived from a patient treated with first-line osimertinib for 8 months. At progression, MSK-IMPACT identified acquired *MET* amplification and *MET* H1094Y. Mutational signature analysis of the osimertinib-naïve and -resistant paired samples for this patient revealed APOBEC mutagenesis restricted to the dominant clone in the osimertinib-resistant sample (Clone 3). Clone 3 harbored a *MET* H1094Y mutation, which is due to a nucleotide level T(C$>$T)A transition mutation that occurs in the APOBEC-preferred mutational context.

Circos plot of the osimertinib-resistant sample also demonstrates that APOBEC-rich genomic areas co-localize with kataegis and other structural rearrangements (tandem duplications, deletions, inversions, and translocations). Similar findings are shown in case WGS-03 (Figure 3B), a patient treated with first-line osimertinib and bevacizumab on a clinical trial for 19 months followed by disease progression; a mechanism of resistance was not identified. Consistent with the findings in WGS-02, clonal decomposition analysis of WGS-03 revealed the emergence of a post-therapy subclone (Clone 3) with a dominant APOBEC mutational signature, which was not observed before osimertinib treatment. These two cases suggest that, in a subset of patients, APOBEC mutagenesis may underpin the acquisition of resistance to osimertinib as observed in other tumors treated with targeted therapies.[34] Clones selected for upon osimertinib treatment harbor repertoires of somatic mutations and structural rearrangements distinct from those of the dominant pretreatment clones, and the development of these new clones may be driven by the acquisition of mutagenic processes (e.g. APOBEC) that were not operative during the early stages of tumorigenesis.

Mechanism of resistance to osimertinib in EGFR-mutant LUADs

We sought to assess the relationship between mutational signatures such as APOBEC and established mechanisms of resistance to osimertinib. Tumors were classified into the following categories of resistance: lineage plasticity (small-cell or squamous transformation), off-target (e.g. acquired fusions and *MET* amplification), on-target (*EGFR*-mediated), and unknown. Tumors were considered to be APOBEC-enriched if either the osimertinib-naïve or -resistant sample was APOBEC dominant. Lineage plasticity and off-target mechanisms of resistance had the highest proportions of APOBEC-enriched samples (56% lineage plasticity, 41% off-target, 24% unknown, 23% on-target, Figure 4A), corroborating the association between APOBEC and lineage plasticity previously reported by our group and others.[13,14] Specifically, most cases of acquired fusions (3/5, 60%) and lineage plasticity (9/16, 56%) had APOBEC as the dominant mutational signature (Figure 4B). Based on the type of substitution and its trinucleotide context, none of the acquired oncogenic mutations were directly attributable to APOBEC mutagenesis except for the case with an acquired MET H1094Y. There were no associations between pretreatment or post-treatment mutational signature and OS (Supplementary Figure S5A-D, available at https://doi.org/10.1016/j.annonc.2022.09.151). Exploration with a larger number of samples is warranted to investigate the relationship between APOBEC mutagenesis and certain mechanisms of resistance, including lineage plasticity and acquired structural rearrangements.

DISCUSSION

In this report, we surveyed mutational signatures in LUADs and identified an association between APOBEC mutagenesis and RTK-driven cancers. We demonstrate that the APOBEC mutational signature can be derived from a routine multigene panel test (i.e. MSK-IMPACT) obtained as the standard

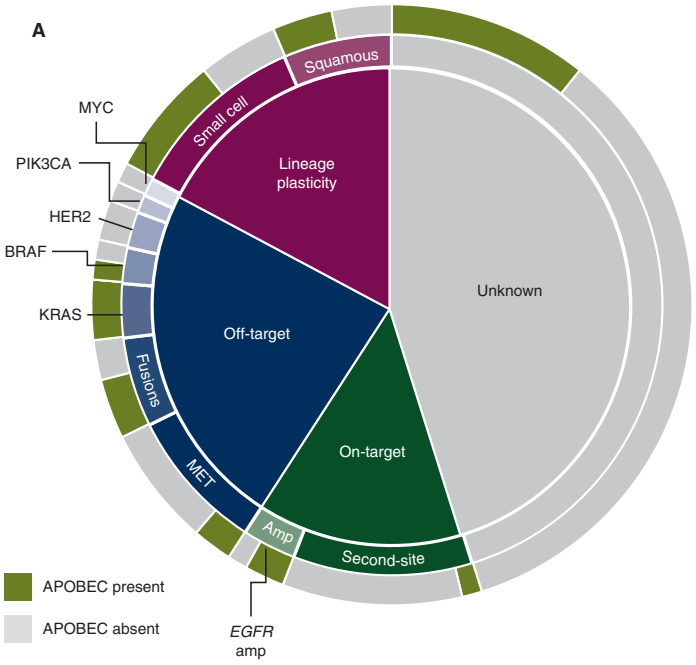

B

Paired pre/post osimertinib IMPACT samples			
	APOBEC signature	Dominant	Non-dominant
Mechanism of resistance	**Cohort size**	**31**	**62**
On-target	*EGFR* amp	2	1
	EGFR C797X	1	7
	EGFR G724S	0	1
	EGFR L718V	0	1
	Total	3	10
Off-target	*BRAF V600E*	1	1
	ERBB2 amp	0	2
	KRAS G12X	3	0
	MET amp	2	3
	MET/EGFR amp	0	1
	MET/ERBB2 amp	0	1
	MET exon 14 skipping	0	1
	MYC amp	0	1
	PIK3CA H1047R	0	1
	EML4-ALK fusion	2	0
	TRIM24-BRAF fusion	1	0
	ZC3HAV1-BRAF fusion	0	1
	RUFY2-RET fusion	0	1
	Total	9	13
Lineage plasticity	Small cell	6	4
	Squamous cell	3	3
	Total	9	7
Unknown	Unknown	10	32

Figure 4. Correlations between APOBEC and acquired resistance in *EGFR*-mutant lung adenocarcinomas. (A) For 93 paired pre- and post-osimertinib samples, mechanism of resistance subgroup (on-target, off-target, lineage plasticity, and unknown) and specific alteration acquired were correlated with the presence of dominant APOBEC signature in either pre- or post-osimertinib sample. (B) Table displaying specific acquired molecular alteration and APOBEC status.
APOBEC, apolipoprotein b mRNA-editing enzyme, catalytic polypeptide-like; EGFR, epidermal growth factor receptor.

of care in patients with metastatic LUADs. Mutational signatures offer an additional layer of genomic information that may clarify how tumors adapt to selective pressure on a genome-wide level, providing a broader perspective on resistance and nominating interventional strategies that could result in more durable suppression of tumor growth. Although WGS remains the 'gold standard' for mutational signature decomposition, WGS or WES data is costly and may require specialized core facilities or additional patient materials. In contrast, the methodology described in this study is based upon sequencing data already routinely obtained for care of patients in the clinic. In fact, in a way akin to how TMB and microsatellite instability are now widely reported on commercial multigene panel testing, other mutational signatures, including APOBEC, could become clinically reportable and provide actionable results in the future.

Our data demonstrate that APOBEC mutagenesis, although present in osimertinib-naïve samples, appears to occur relatively late in the development and progression of LUADs and increases with osimertinib exposure, with enrichment in metastatic tumors and subclonal as well as private mutations. Such findings are corroborated by preclinical work that EGFR or ALK inhibitor treatment induces expression and mutagenic activity of APOBEC3B in tumor xenograft models and cell lines.[35] Separately, inhibiting therapy-induced APOBEC3A mutagenesis by gene deletion or RNA inhibitor-meditated suppression in lung cancer cell lines delayed resistance to targeted therapies.[36] Identifying a role for APOBEC mutagenesis in mediating drug resistance presents opportunities for abrogating the development of such resistance by potentially focusing on APOBEC inhibition, an area of active investigation.[37-39] While there are currently no direct inhibitors for APOBEC activity, previous studies[40,41] have proposed a potential role for ataxia telangiectasia and Rad3-related (ATR) and PARP inhibitors. Preclinical studies demonstrate that activation of APOBEC-3A and APOBEC-3B may sensitize tumor cells to DNA damage response pathway inhibitors, such as ATR and PARP inhibitors; *in vitro* studies have shown that ATR inhibition can overcome osimertinib resistance in some cases.[42]

Consistent with previous observations,[32] our data demonstrate that APOBEC mutagenesis is associated with kataegis and chromothripsis.[43] These phenomena can increase the probability of translocations leading to activating gene fusions that can drive resistance to EGFR TKIs. The association between APOBEC and lineage plasticity can be considered in analogy with simpler organisms, as lineage plasticity mirrors phenotypic switching seen in bacteria following antibiotic exposure.[44] In bacteria, larger-scale genomic processes with functional similarities to APOBEC mutagenesis, including slipped strand repair, homologous recombination, site-specific recombination, and transposon insertion and excision can all induce phenotypic switching.[45] APOBEC-derived catastrophic genomic events such as chromothripsis may result in profound reprogramming of cancer cells, creating a milieu that is conducive for phenotypic plasticity and resultant drug resistance. Alternatively, APOBEC mutagenesis may result in greater clonal diversity, providing the required conditions for the selection of de-differentiated subclones that have gained histologic plasticity.

https://doi.org/10.1016/j.annonc.2022.09.151

This study has several limitations. Although WGS analysis was carried out for a subset of pre- and post-osimertinib treated samples, mutational signature decomposition was largely carried out by applying SigMA to MSK-IMPACT-targeted sequencing data. Despite the agreement between MSK-IMPACT and WES using SigMA for the detection of APOBEC mutagenesis, our analysis may have overestimated the extent of APOBEC exposure across samples from all groups analyzed.

Indeed, the five SNVs cut-off applied for the inclusion of samples in our mutational signature analysis was found to display ~75% specificity against the gold-standard WES. The specificity, however, was higher when ≥10 and ≥15 SNVs were used as cut-off values (86% and 85%, respectively). Nonetheless, the inclusion of only samples with >10 SNVs would result in the exclusion of a large proportion of samples from the analysis, inevitably creating a selection bias for LUADs with higher mutation burden. Due to limited availability of paired tumor samples obtained before and after a given treatment, we did not investigate whether APOBEC enrichment following targeted therapy would also occur in the context of chemotherapy and immunotherapy treatment. In fact, here we focused on EGFR-mutant lung cancer; the analysis of other RTK driver lung cancers, including *ALK-*, *RET-,* and *ROS1*-positive lung cancers, in sufficiently powered cohorts should be entertained in future studies.

Although the mechanistic basis for the induction of APOBEC mutagenesis in cancer cells and the causes of the selective enrichment for this phenomenon in certain clinical contexts remains to be fully elucidated, the association with RTK-driven lung cancers, targeted therapy exposure, and selected mechanisms of resistance provide clear directions for further study. APOBEC mutagenesis appears to constitute a transient, intermittent process,[16] and deciphering the factors that induce and suppress episodic APOBEC mutagenesis during cancer evolution may inform whether this process might be harnessed therapeutically. Mutational signatures as a biomarker for treatment have been established with homologous repair deficiency and microsatellite instability, which can select patients for treatment with DNA-damaging agents[46] and immunotherapy, respectively. The value of mutational signatures is heightened by the ability to infer signatures from multigene panel sequencing, which is frequently obtained for routine clinical care for patients with LUADs; at present, however, detecting APOBEC mutagenesis clinically is not warranted for lung cancer patients. Ultimately, the clinical relevance of APOBEC mutagenesis centers around therapeutic vulnerability. Future studies focusing on the development of approaches seeking to prevent the development of resistance by blocking the APOBEC mutagenesis process as well synthetic lethal approaches specifically targeting cancer cells with active APOBEC mutagenesis are warranted.

FUNDING

SC was supported by the National Cancer Institute [grant numbers NCI-P50CA247749, NCI-R01CA249666]; CML was supported in part by EGFR Resisters/LUNGevity Lung Cancer Research Award and GO2 Foundation ALK Positive Research Award [grant numbers R01CA227833, P30-CA086485, UG1CA233259, P01CA129243]; HAY was supported in part by EGFR Resisters/LUNGevity Lung Cancer Research Award and STARR foundation [grant number R01CA264078]. MSK authors were supported by the National Cancer Institute Cancer Center Core [grant number P30-CA008748].

DISCLOSURE

NJC received honoraria from MJH Life Sciences; royalties from Wolters Kluwer (Pocket Oncology). MFB reports a consulting or advisory role for Roche, Eli Lilly, PetDx; research funding from Grail. ML reports a consulting or advisory role for Takeda Oncology, Janssen Pharmaceuticals. CMR reports a consulting or advisory role for AbbVie, Amgen, Astra Zeneca, Epizyme, Genentech/Roche, Ipsen, Jazz, Lilly, and Syros; serves on the scientific advisory boards of Bridge Medicines, Earli, and Harpoon Therapeutics. SC reports a consulting or advisory role: Novartis, Lilly, Sanofi, Paige.AI Research Funding: Daiichi Sankyo (Inst), Paige.AI (Inst) Patents, Royalties, Other Intellectual Property: Patents for (1) targeting mutant estrogen receptor (ER) with ER proteolysis targeting chimera (PROTACS) and (2) detecting genomic and histologic alterations in breast cancer using machine learning algorithms (Inst) Travel, Accommodations, Expenses: Bristol Myers. CML is a consultant/advisory board member for Pfizer, Novartis, AstraZeneca, Genoptix, Sequenom, Ariad, Takeda, Blueprints Medicine, Cepheid, Foundation Medicine, Roche, Achilles Therapeutics, Genentech, Syros, Amgen, EMD-Serono, Eli Lilly, Daiichi-Sanko, and PUMA and has received research grants (to her University) from Xcovery, AstraZeneca, and Novartis. None of the grants are active at this time. JSR-F reports receiving personal/consultancy fees from Goldman Sachs, REPARE Therapeutics, Paige.AI and Eli Lilly, membership of the scientific advisory boards of VolitionRx, REPARE Therapeutics, Paige.AI and Personalis, membership of the Board of Directors of Grupo Oncoclinicas, and ad hoc membership of the scientific advisory boards of Roche Tissue Diagnostics, Ventana Medical Systems, Novartis, Genentech, MSD, Daiichi Sankyo and InVicro, outside the scope of this study and owns Paige.AI and REPARE Therapeutics stocks. HAY reports consultant or advisory role for AstraZeneca, Janssen, Blueprint Med, C4 Therapeutics, and Daiichi. Research funding: AstraZeneca (Inst), Pfizer (Inst), Daiichi (Inst), Cullinan (Inst), Lilly (Inst), and Novartis (Inst). All other authors have declared no conflicts of interest.

REFERENCES

1. Schoenfeld AJ, Chan JM, Kubota D, et al. Tumor analyses reveal squamous transformation and off-target alterations as early resistance mechanisms to first-line osimertinib in EGFR-mutant lung cancer. *Clin Cancer Res*. 2020;26:2654-2663.
2. Roper N, Brown AL, Wei JS, et al. Clonal evolution and heterogeneity of osimertinib acquired resistance mechanisms in EGFR mutant lung cancer. *Cell Rep Med*. 2020;1:100007.

3. de Bruin EC, McGranahan N, Mitter R, et al. Spatial and temporal diversity in genomic instability processes defines lung cancer evolution. *Science*. 2014;346:251-256.
4. Swanton C, McGranahan N, Starrett GJ, Harris RS. APOBEC Enzymes: mutagenic fuel for cancer evolution and heterogeneity. *Cancer Discov*. 2015;5:704-712.
5. Zhang J, Fujimoto J, Zhang J, et al. Intratumor heterogeneity in localized lung adenocarcinomas delineated by multiregion sequencing. *Science*. 2014;346:256-259.
6. André T, Shiu KK, Kim TW, et al. Pembrolizumab in microsatellite-instability—high advanced colorectal cancer. *N Engl J Med*. 2020;383:2207-2218.
7. Marcus L, Lemery SJ, Keegan P, Pazdur R. FDA approval summary: pembrolizumab for the treatment of microsatellite instability-high solid tumors. *Clin Cancer Res*. 2019;25:3753-3758.
8. González-Martín A, Pothuri B, Vergote I, et al. Niraparib in patients with newly diagnosed advanced ovarian cancer. *N Engl J Med*. 2019;381:2391-2402.
9. Longo DL. Personalized medicine for primary treatment of serous ovarian cancer. *N Engl J Med*. 2019;381:2471-2474.
10. Mirza MR, Monk BJ, Herrstedt J, et al. Niraparib maintenance therapy in platinum-sensitive, recurrent ovarian cancer. *N Engl J Med*. 2016;375:2154-2164.
11. Soria JC, Ohe Y, Vansteenkiste J, et al. Osimertinib in untreated EGFR-mutated advanced non-small-cell lung cancer. *N Engl J Med*. 2018;378:113-125.
12. Leonetti A, Sharma S, Minari R, Perego P, Giovannetti E, Tiseo M. Resistance mechanisms to osimertinib in EGFR-mutated non-small cell lung cancer. *Br J Cancer*. 2019;121:725-737.
13. Lee JK, Lee J, Kim S, et al. Clonal history and genetic predictors of transformation into small-cell carcinomas from lung adenocarcinomas. *J Clin Oncol*. 2017;35:3065-3074.
14. Offin M, Chan JM, Tenet M, et al. Concurrent RB1 and TP53 alterations define a subset of EGFR-mutant lung cancers at risk for histologic transformation and inferior clinical outcomes. *J Thorac Oncol*. 2019;14:1784-1793.
15. Venkatesan S, Rosenthal R, Kanu N, et al. Perspective: APOBEC mutagenesis in drug resistance and immune escape in HIV and cancer evolution. *Ann Oncol*. 2018;29:563-572.
16. Petljak M, Alexandrov LB, Brammeld JS, et al. Characterizing mutational signatures in human cancer cell lines reveals episodic APOBEC mutagenesis. *Cell*. 2019;176:1282-1294.e1220.
17. McGranahan N, Favero F, de Bruin EC, Birkbak NJ, Szallasi Z, Swanton C. Clonal status of actionable driver events and the timing of mutational processes in cancer evolution. *Sci Transl Med*. 2015;7. 283ra254.
18. Gulhan DC, Lee JJ, Melloni GEM, Cortés-Ciriano I, Park PJ. Detecting the mutational signature of homologous recombination deficiency in clinical samples. *Nat Genet*. 2019;51:912-919.
19. Cheng DT, Mitchell TN, Zehir A, et al. Memorial Sloan Kettering-integrated mutation profiling of actionable cancer targets (MSK-IMPACT): a hybridization capture-based next-generation sequencing clinical assay for solid tumor molecular oncology. *J Mol Diagn*. 2015;17:251-264.
20. Zehir A, Benayed R, Shah RH, et al. Mutational landscape of metastatic cancer revealed from prospective clinical sequencing of 10,000 patients. *Nat Med*. 2017;23:703-713.
21. Shen R, Seshan VE. FACETS: allele-specific copy number and clonal heterogeneity analysis tool for high-throughput DNA sequencing. *Nucleic Acids Res*. 2016;44:e131.
22. Carter SL, Cibulskis K, Helman E, et al. Absolute quantification of somatic DNA alterations in human cancer. *Nat Biotechnol*. 2012;30:413-421.
23. Ng CKY, Piscuoglio S, Geyer FC, et al. The landscape of somatic genetic alterations in metaplastic breast carcinomas. *Clin Cancer Res*. 2017;23:3859-3870.
24. Weigelt B, Bi R, Kumar R, et al. The landscape of somatic genetic alterations in breast cancers from ATM germline mutation carriers. *J Natl Cancer Inst*. 2018;110:1030-1034.
25. Guo Q, Lakatos E, Al Bakir I, Curtius K, Graham TA, Mustonen V. The mutational signatures of formalin fixation on the human genome. *bioRxiv*. 2021.
26. Alexandrov LB, Nik-Zainal S, Wedge DC, et al. Signatures of mutational processes in human cancer. *Nature*. 2013;500:415-421.
27. Alexandrov LB, Kim J, Haradhvala NJ, et al. The repertoire of mutational signatures in human cancer. *Nature*. 2020;578:94-101.
28. Mayakonda A, Lin DC, Assenov Y, Plass C, Koeffler HP. Maftools: efficient and comprehensive analysis of somatic variants in cancer. *Genome Res*. 2018;28:1747-1756.
29. Gu Z, Eils R, Schlesner M. Complex heatmaps reveal patterns and correlations in multidimensional genomic data. *Bioinformatics*. 2016;32:2847-2849.
30. Roper N, Gao S, Maity TK, et al. APOBEC mutagenesis and copy-number alterations are drivers of proteogenomic tumor evolution and heterogeneity in metastatic thoracic tumors. *Cell Rep*. 2019;26:2651-2666.e2656.
31. Gerstung M, Jolly C, Leshchiner I, et al. The evolutionary history of 2,658 cancers. *Nature*. 2020;578:122-128.
32. Maciejowski J, Chatzipli A, Dananberg A, et al. APOBEC3-dependent kataegis and TREX1-driven chromothripsis during telomere crisis. *Nat Genet*. 2020;52:884-890.
33. Nik-Zainal S, Alexandrov LB, Wedge DC, et al. Mutational processes molding the genomes of 21 breast cancers. *Cell*. 2012;149:979-993.
34. Van Allen EM, Wagle N, Sucker A, et al. The genetic landscape of clinical resistance to RAF inhibition in metastatic melanoma. *Cancer Discov*. 2014;4:94-109.
35. Mayekar MK, Caswell DR, Vokes NI, et al. Targeted cancer therapy induces APOBEC fuelling the evolution of drug resistance. *bioRxiv*. 2020.
36. Isozaki H, Abbasi A, Nikpour N, et al. APOBEC3A drives acquired resistance to targeted therapies in non-small cell lung cancer. *bioRxiv*. 2021.
37. Olson ME, Harris RS, Harki DA. APOBEC enzymes as targets for virus and cancer therapy. *Cell Chem Biol*. 2018;25:36-49.
38. Matsumoto T, Shirakawa K, Yokoyama M, et al. Protein kinase A inhibits tumor mutator APOBEC3B through phosphorylation. *Sci Rep*. 2019;9:8307.
39. Kvach MV, Barzak FM, Harjes S, et al. Inhibiting APOBEC3 activity with single-stranded DNA containing 2'-deoxyzebularine analogues. *Biochemistry*. 2019;58:391-400.
40. Green AM, Budagyan K, Hayer KE, et al. Cytosine deaminase APOBEC3A sensitizes leukemia cells to inhibition of the DNA replication checkpoint. *Cancer Res*. 2017;77:4579-4588.
41. Buisson R, Lawrence MS, Benes CH, Zou L. APOBEC3A and APOBEC3B activities render cancer cells susceptible to ATR inhibition. *Cancer Res*. 2017;77:4567-4578.
42. Tanaka K, Yu HA, Yang S, et al. Targeting Aurora B kinase prevents and overcomes resistance to EGFR inhibitors in lung cancer by enhancing BIM- and PUMA-mediated apoptosis. *Cancer Cell*. 2021;39:1245-1261.e1246.
43. Nik-Zainal S, Alexandrov LB, Wedge DC, et al. Mutational processes molding the genomes of 21 breast cancers. *Cell*. 2012;149:979-993.
44. Chantratita N, Wuthiekanun V, Boonbumrung K, et al. Biological relevance of colony morphology and phenotypic switching by *Burkholderia pseudomallei*. *J Bacteriol*. 2007;189:807-817.
45. Sousa AM, Machado IM, Pereira MO. Phenotypic switching: an opportunity to bacteria thrive. *Science Against Microbial Pathogens: Communicating Current Research and Technological Advances*. 2011:252-262.
46. Mukhopadhyay A, Plummer ER, Elattar A, et al. Clinicopathological features of homologous recombination-deficient epithelial ovarian cancers: sensitivity to PARP inhibitors, platinum, and survival. *Cancer Res*. 2012;72:5675-5682.